Hindawi
International Journal of Antennas and Propagation
Volume 2019, Article ID 5427595, 9 pages
https://doi.org/10.1155/2019/5427595

Research Article

The New C-Shaped Parasitic Strip for the Single-Feed Circularly Polarized (CP) Microstrip Antenna Design

Zhao-Lin Zhang, Kun Wei, Jian Xie, Jian-Ying Li, and Ling Wang

School of Electronics and Information, Northwestern Polytechnical University, Xi'an 710072, China

Correspondence should be addressed to Kun Wei; weikun916@163.com

Received 22 July 2019; Revised 29 September 2019; Accepted 19 October 2019; Published 11 November 2019

Academic Editor: N. Nasimuddin

A new single-feed circularly polarized (CP) microstrip antenna with the C-shaped parasitic strip is proposed in this paper. The proposed CP antenna is designed for the transmitting terminal in the Global Navigation Satellite System (GNSS). The square patch is surrounded by a C-shaped parasitic strip. By adjusting the parasitic strip dimension, the antenna CP operation is achieved. The main advantage of this method is that those two resonant modes for achieving the CP operation are independent from each other, which is liable to design and debug the proposed CP microstrip antenna. The designed CP microstrip antenna has the good impedance matching, the good CP radiation pattern, and the stable CP gain across the 3 dB AR (axial ratio) bandwidth.

1. Introduction

The CP antenna is extensively used in the Global Navigation Satellite System (GNSS) because of its advantages for improving the system sensitivity and reducing the polarization mismatch. There are many kinds of CP antennas, like microstrip antenna, horn antenna, and helix antenna. Microstrip antenna is widely used in both military and civil applications because of the following advantages: small size, low cost, easy to be manufactured, and convenient to expand into arrays [1]. For a square-radiated patch antenna, one easy way to achieve CP operation is feeding the patch at two orthogonal directions to excite two resonant modes. However, the dual-feeding mechanism enlarges the antenna dimension, increases the antenna geometry complexity, and leads to extra loss. To overcome the dual-feeding complexities, the square patch antenna with the single-feed port has been studied [2]. The single-feed microstrip antenna has the simplest structure for achieving the CP radiation.

With the development of the GNSS, various single-feed CP microstrip antennas achieved by adjusting the patch physical dimensions or etching the slots have been reported. A CP antenna for the GNSS application is presented in [3]. The antenna CP operation is achieved by feeding network. A novel low-profile CP microstrip antenna is proposed in [4]. The antenna consists of two circular eccentric rings for achieving the CP operation, which are simultaneously excited by an arc-shaped strip. The CP microstrip antennas based on the fractal boundary are proposed in [5, 6]. By replacing the sides of a square patch with asymmetrical prefractal curves, two orthogonal modes are excited for CP operation. A single-feed microstrip antenna with loading of shorting pins for CP radiation is proposed in [7]. After the optimal loading position is investigated for maximum directivity of the linear polarization, one pair of the inner pins is slightly shifted in an offset to properly separate the two degenerate modes, so that the CP radiation can be excited. An asymmetric-circular shaped slotted microstrip antenna with slits is proposed in [8] for the CP radiation. The single-feed configuration based asymmetric-circular shaped slotted square microstrip patches are adopted to realize the CP microstrip antenna. A compact CP-stacked patch antenna is investigated for BeiDou navigation satellite system in [9]. The bottom patch with symmetrical slant cornercuts and the top one with two rectangular stubs on the diagonal produce a pair of degenerated modes, achieving CP radiation.

A microstrip antenna with the CP radiation is proposed and investigated in [10]. The patch has an octagon-star shape

and can be considered as a superimposition of two square patches. By generating two orthogonal degenerated TM_{11} modes from the two superimposed square patches, the CP radiation is achieved. It is demonstrated in [11] that by introducing a reconfigurable C-shaped slot in a circular patch antenna, the CP radiation of the antenna is obtained. A novel CP antenna for GNSS application based on the mode analysis on the shorting load patch is proposed in [12]. By adjusting the position and the size of the shorting load structure, the dominant resonant mode of the patch antenna (TM_{10}) is divided into two secondary modes. A novel annular slotted center-feed CP antenna is proposed in [13]. Two symmetric annular slots with tabs are embedded onto a square microstrip patch for the CP radiation. The antenna composed of a loop feeding structure, four driven patches, and four parasitic patches is proposed in [14]. The driven patches, which are capacitively coupled by the feeding loop, generate the CP mode due to the sequentially rotated structure and four parasitic patches.

A CP antenna fed by four apertures is introduced in [15]. A lotus-shaped aperture is added to optimize the coupling between the microstrip lines, and the rings are used for achieving the CP radiation. A single-feed arrowhead-shaped slotted microstrip antenna for the CP operation is proposed in [16]. The arrowhead-shaped slot is embedded in the first quadrant along the diagonal axes of a square patch to achieve the CP operation. A low-profile dual-band CP microstrip antenna is proposed in [4]. The antenna consists of two circular eccentric rings with different sizes. Two eccentric rings each work as a single-band circular polarization radiator and are simultaneously excited by an arc-shaped strip. A CP microstrip antenna with conical-beam radiation is presented in [17]. The antenna is excited at the second-order mode to generate the conical radiation pattern and fed by a hybrid coupler to obtain the CP operation, which shows a stable performance with varisized metal reflectors.

Some CP antennas achieved by the parasitic structure have been reported. The antenna CP operation in [18] is achieved by adding the parasitic DGS (defected ground structure) in the ground plane. However, the DGS will increase the antenna backward radiation. A CP square patch antenna is presented in [19]. To achieve the CP radiation, the square patch is embedded with a cross slot and an L-shaped open-end microstrip line. The antenna in [20] consists of a radiating patch and two separated parasitic strips, and the separated strips are placed at the outer perimeter of the patch for capacitive coupling. The antenna CP operation is achieved by moving the separated positions of the strips. Table 1 lists the comparisons of this work and previous published CP antennas. It shows the proposed CP antenna achieved by the parasitic strip in this paper has a simple structure and the independent resonant modes.

This paper presents a novel CP microstrip antenna achieved by a C-shaped parasitic strip. The proposed CP antenna consists of a square patch and a simple C-shaped parasitic strip. By adjusting the parasitic strip dimension, two orthogonal modes will have the equal amplitudes and 90 deg phase difference for achieving the CP operation. The designed CP microstrip antenna has the good impedance matching, the good CP radiation patterns, and the stable CP gain across the 3 dB AR bandwidth. The resonant modes for achieving the proposed CP antenna are independent from each other, which is convenient for the CP antenna design and debug.

2. Antenna Geometries

The geometries of the proposed CP microstrip antenna, as well as the C-shaped parasitic strip are drawn in Figure 1. The designed CP antenna resonates at the center frequency 1.65 GHz. Both the square patch and the parasitic strip are printed on a substrate with the dielectric constant 10, height 3.18 mm, and loss tangent 0.0035. Antenna element has outline dimension 65 mm. The square patch is fed by a coaxial probe, which has the distance d away from the patch edge. The length of the square patch is l. A C-shaped parasitic strip surrounds the radiated patch, which is applied for realizing the CP operation. The parasitic strip has width w and total length $l = l1 + l2 + l3 + l4$. The gap width between the radiated patch and the parasitic strip is g.

To understand the antenna CP design principle, Figure 2 shows the surface current vector graphs at the frequency 1.65 GHz of the radiated patch with the C-shaped parasitic strip at different time phases (ωt), from 0° to 270° with an interval of 90°. The current vectors at the frequency 1.65 GHz are only detected in the horizontal direction before adding the C-shaped parasitic strip. When adding the C-shaped parasitic strip, the new current vectors are detected in the vertical direction, as shown in subgraphs (a) and (c). It clearly shows that the second resonant mode is generated because of the asymmetric C-shaped parasitic strip structure, which helps to achieve the CP design. By adjusting the parasitic strip dimension, these two orthogonal resonant modes will have the approximately equal amplitude value and 90 deg time-phase difference, which contributes to achieve the CP operation. Moreover, the surface current vector rotation is counterclockwise, which means the proposed microstrip antenna is left-handed circularly polarized. By mirroring the parasitic strip along the y-axis, the antenna circular polarization can be transformed from LHCP to RHCP, as shown in the Figure 3.

By introducing a proper asymmetry in the structure, the degeneracy can be removed with one mode increasing with frequency, while the orthogonal mode will be decreasing with frequency by the same amount. Since the two modes will have slightly different frequencies, by proper design, the field of one mode can lead by 90 deg phase difference necessary for circular polarization. For the CP antenna in this paper, the asymmetry parasitic structure generates the second resonant mode, which has a slightly different frequency and the 90 deg phase difference with the original resonant mode. Due to that, the antenna CP radiation is realized.

3. Antenna Parametric Analysis

To better illustrate how the antenna CP operation is realized, the parameter studies of the C-shaped parasitic strip are

Table 1: Comparison of this work and previous published CP antennas.

Ref.	Method to achieve the CP operation	Dielectric constant	Operating frequency	10 dB BW	3 dB AR BW	Antenna size	Network required	Independent resonant modes
[3]	Feeding network	2.33	1.575 GHz	N.A.	N.A.	$\phi 0.61\lambda_0 \times 0.008\lambda_0$	Yes	No
[5]	Fractal structure	2.2	2.54 GHz	6.4%	2%	$0.35\lambda_0 \times 0.35\lambda_0 \times 0.027\lambda_0$	No	No
[7]	Metallic pins	2.2	2.53 GHz	4.3%	1.15%	$1.26\lambda_0 \times 1.26\lambda_0 \times 0.027\lambda_0$	No	No
[9]	Rectangular stubs	4.4	1.615 GHz	9.1%	1%	$0.38\lambda_0 \times 0.38\lambda_0 \times 0.024\lambda_0$	No	No
[10]	Octagon-star shaped patch	2.164	1.575 GHz	2.5%	0.5%	$\varphi 0.42\lambda_0 \times 0.016\lambda_0$	No	No
[12]	Feeding network	6	1.35 GHz	32%	32%	$0.2\lambda_0 \times 0.2\lambda_0 \times 0.005\lambda_0$	Yes	No
[18]	DGS	10	1.575 GHz	1.9%	0.4%	$0.24\lambda_0 \times 0.24\lambda_0 \times 0.017\lambda_0$	No	Yes
[19]	Two parasitic strips	4.4	925 MHz	5.4%	0.65%	$0.22\lambda_0 \times 0.22\lambda_0 \times 0.005\lambda_0$	No	No
This work	Single C-shaped parasitic strip	10	1.65 GHz	1.9%	0.61%	$0.36\lambda_0 \times 0.36\lambda_0 \times 0.017\lambda_0$	No	Yes

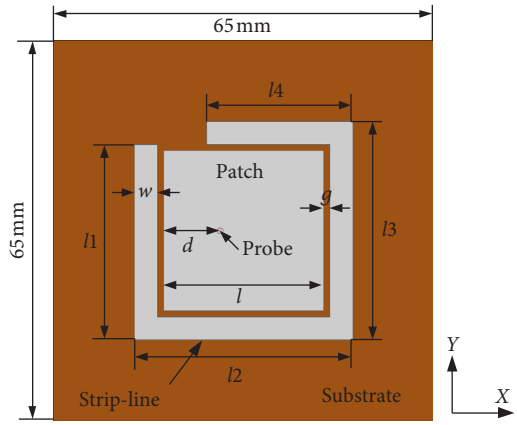

Figure 1: The geometries of the designed CP microstrip antenna.

carried out. To simplify the study process, the gap width between the patch and the parasitic strip is fixed to be 1 mm. By optimizing the C-shaped parasitic strip dimension, the better antenna CP performance is achieved. The optimized parameter values of the designed CP microstrip antenna are $l1 = 33.4$ mm, $l2 = 37.4$ mm, $l3 = 37.4$ mm, $l4 = 25$ mm, $w = 4$ mm, $l = 27.4$ mm, $d = 9.7$ mm, and $g = 1$ mm.

Figures 4 and 5 show S11 and the axial ratio (AR) of the designed CP antenna when tuning the parasitic strip length $l4$. It clearly shows that the proposed CP antenna achieved by the C-shaped parasitic strip has two resonant modes. One resonant mode is fixed in the high-frequency region, and the other resonant mode moves to the low-frequency region when increasing the parasitic strip length. Because there is no patch dimension change, the resonant mode in the x-axis is fixed in the high-frequency region. The other resonant mode is determined by the electric field E_y in the y-direction, which is generated by the vertical current distributions. This second resonant mode moves to the lower frequency region when increasing the parasitic strip length. By optimizing the parasitic strip length, these two resonant modes in the orthogonal direction will have the same magnitude and 90° time-phase difference. Due to that, the antenna CP radiation is realized. Figure 4 gives the proposed CP antenna AR against theta, when tuning the parasitic length $l4$. When the parasitic length $l4$ equals to 25 mm, the proposed antenna has better CP performances.

Figures 6 and 7 show S11 and the axial ratio (AR) of the designed CP antenna when tuning the gap width g. Figure 5 clearly shows that the proposed CP antenna has two resonant modes. One of the resonant modes moves to the high-frequency region when increasing the gap width. Because there is no patch dimension change, the resonant mode in the x-axis is fixed in the high-frequency region. The other resonant mode is determined by the electric field E_y in the y-direction, which is generated by the vertical current distributions. Figure 6 gives the proposed CP antenna AR against theta, when turning the gap width g. When the gap width g equals to 1 mm, the proposed antenna has better CP performances. The 3 dB AR beamwidth is approximately 200deg in the phi = 0deg plane.

The C-shaped parasitic strip dimension optimization affects only one resonant mode, which indicates that those two resonant modes for achieving the antenna CP operation are independent from each other. This is the main advantage or novelty of the proposed CP antenna in this paper, which is liable to design and debug the proposed CP antenna.

4. The Optimized Simulation Results

The simulated antenna S11 with and without the C-shaped parasitic strip is drawn in Figure 8 for comparison. Before adding the C-shaped parasitic strip, the bandwidth of the linear polarized (LP) antenna is 20 MHz. When the parasitic strip is added, the antenna polarization is transformed from linear polarization to circular polarization. Moreover, the bandwidth of the CP antenna is expanded to 31 MHz (from 1.635 GHz to 1.666 GHz), which is wider than that of the antenna without the C-shaped parasitic strip. The existent of these two resonant modes results to expand the antenna bandwidth. This also leads to the double minimum in the matching frequency behavior.

Figure 9 shows the simulated radiation patterns in different planes of the designed CP microstrip antenna with the parasitic strip at 1.65 GHz. In both the phi = 0deg and phi = 90deg planes, it shows that the radiation patterns are in the domination position. The proposed CP antenna with the C-shaped parasitic strip has the peak gain 4.2 dBic and efficiency approximately 78%. When enlarging the ground plane to be 100×100 mm^2, the gain of the proposed CP

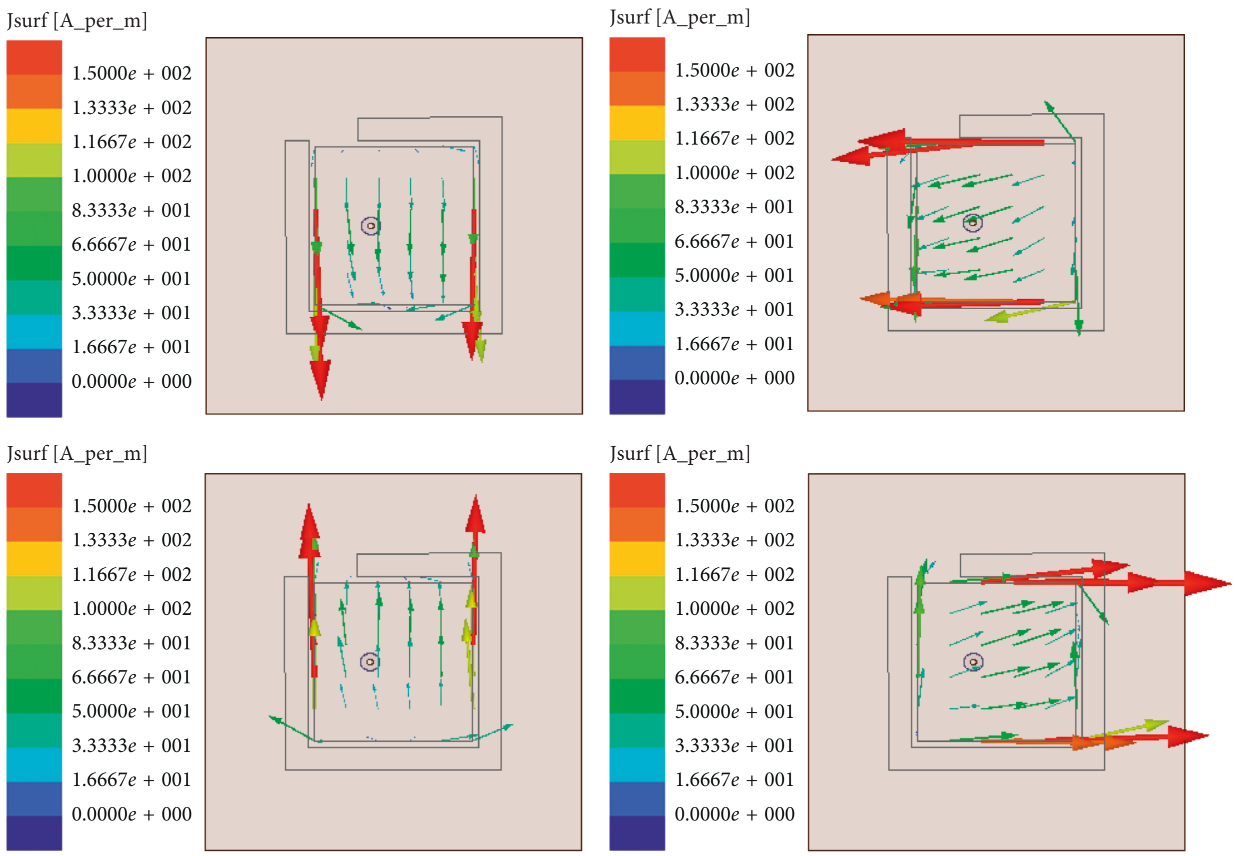

Figure 2: The surface current distribution on the LHCP antenna radiated patch at 1.65 GHz.

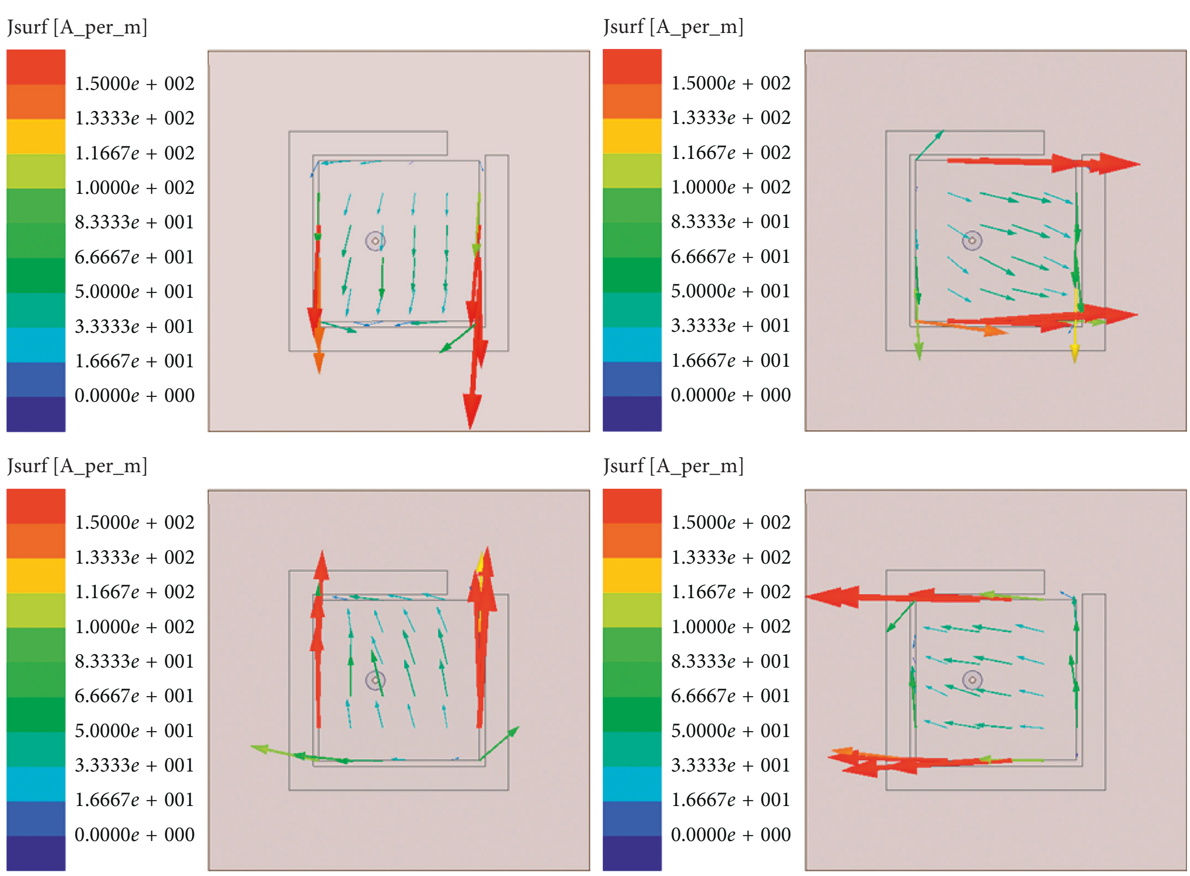

Figure 3: The surface current distribution showing RHCP behavior of the antenna with the mirrored parasitic strip at 1.65 GHz.

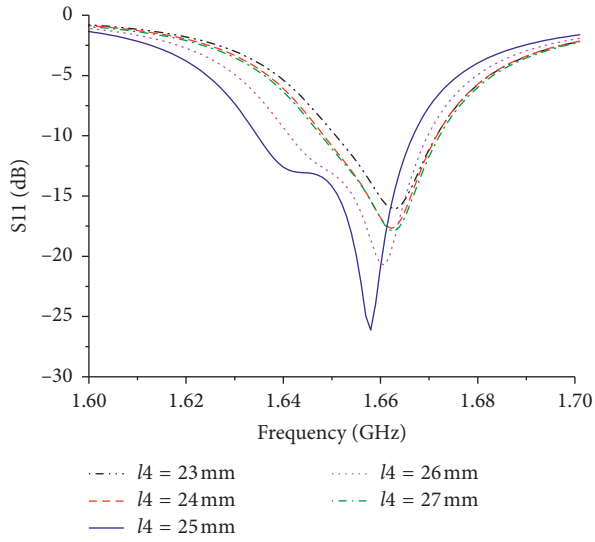

Figure 4: Antenna S11 when tuning the C-shaped parasitic strip length $l4$.

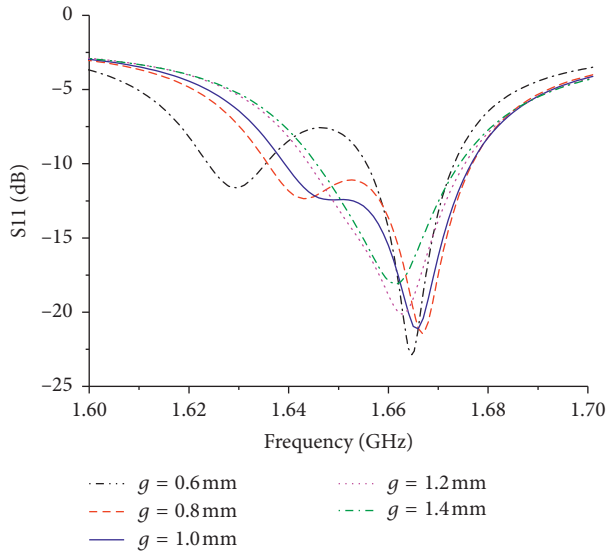

Figure 6: Antenna S11 when tuning the gap width g.

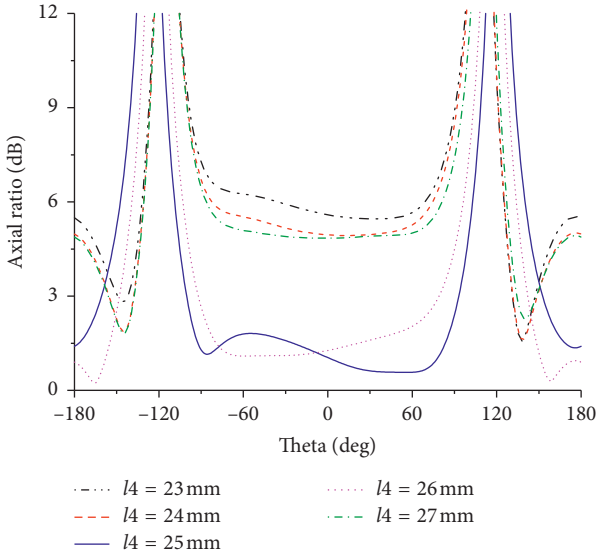

Figure 5: The AR against theta at phi = 0 deg plane when tuning the C-shaped parasitic strip length $l4$.

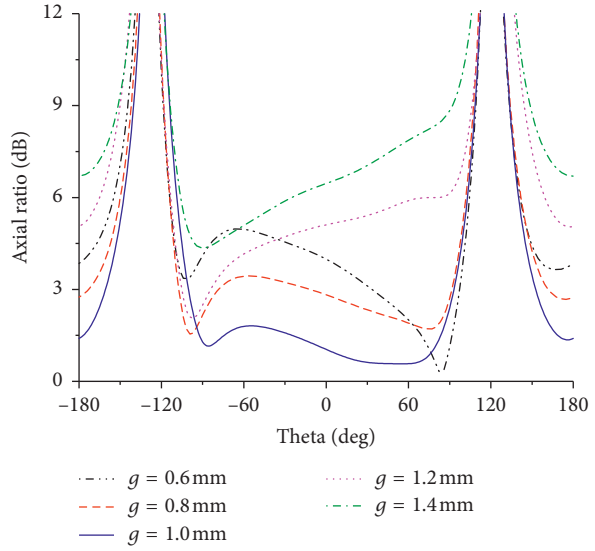

Figure 7: The AR against theta at phi = 0 deg plane when tuning the gap width g.

antenna will be increased from 4.2 dBic to 5.3 dBic, and the backside radiation will be decreased.

Figure 10 illustrates the antenna AR against theta in different planes. The 3 dB AR beamwidth covers the angles from theta = −60deg to theta = 60deg. The minimum value of the AR is 0.7 dB at the center frequency (1.65 GHz), which indicates that the designed antenna has pure circular polarization. In the boresight direction, the AR value is approximately 1 dB. The 3 dB AR beamwidth is approximately 200deg, 190deg, 175deg, and 160deg in the phi = 0, 30, 60, and 90deg planes, respectively.

Figure 11 shows the antenna ARs against frequency with and without the C-shaped parasitic strip. Before adding the parasitic strip, the antenna is linear polarized. So the ARs of the antenna without the parasitic strip are much larger than those of the antenna with the parasitic strip.

5. The Simulation and Measurement Comparisons

The proposed CP microstrip antenna is fabricated based on the optimized parameters. As shown in Figure 12, both the antenna patch and the C-shaped parasitic strip are printed on the substrate with the dielectric constant 10, height 3.18 mm, and loss tangent 0.0035. The simulation and measurement S11 of the CP microstrip antenna are plotted in Figure 13. The measurement result agrees well with the simulation result. Both the simulation and measurement

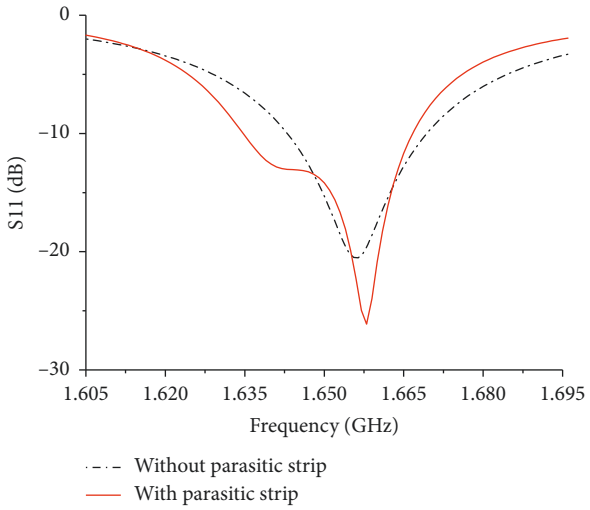

Figure 8: The antenna S11 with and without the C-shaped parasitic strip.

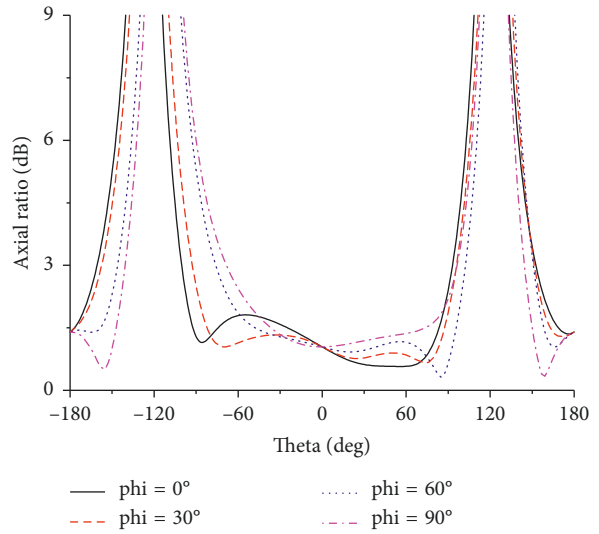

Figure 10: The designed antenna ARs in different planes at center frequency.

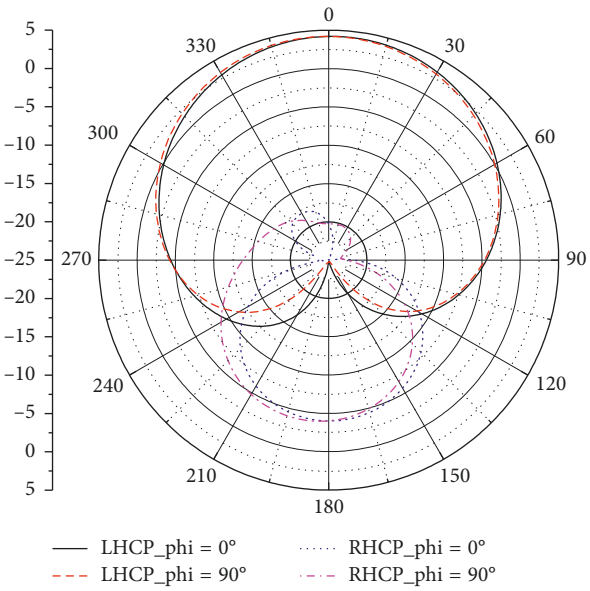

Figure 9: The radiation patterns of the CP antenna with and without the C-shaped parasitic strip.

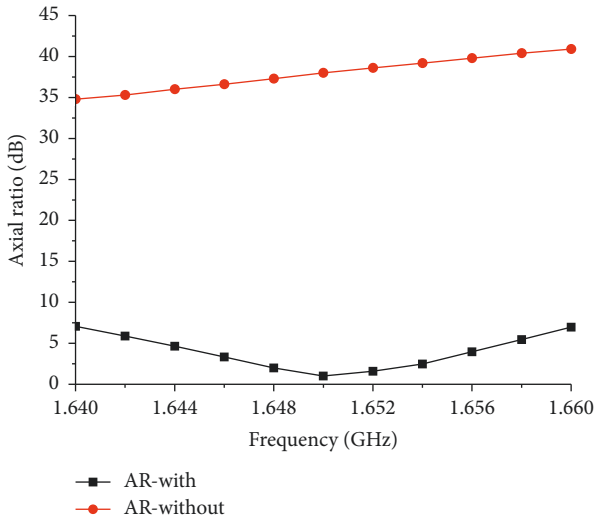

Figure 11: The comparisons of the ARs against frequency with and without the parasitic strip.

results show that the bandwidth of the designed antenna is 30 MHz (1.8% with center frequency 1.65 GHz). The slight differences between the measurement and the simulation may be caused by the machine error of the fabricated CP microstrip antenna.

The simulated and measured radiation patterns of the proposed CP microstrip antenna on both the phi = 0deg and phi = 90deg planes are plotted in Figure 14. The results show that the simulated radiation patterns agree well with the measured ones. It also clearly shows that the proposed antenna presents good broadside radiation patterns. In the upper-sphere space, there are no significant main lobe pattern differences between the simulation and the measurement. The proposed CP microstrip antenna has the peak gain about 4.2 dBic, the 3 dB beamwidth about 90deg, and the antenna efficiency about 78%. Moreover, the cross polarization level is less than −15 dB.

The simulated and measured ARs and CP gains in the boresight direction against frequency are plotted in Figure 15. A reasonable good agreement between the simulation and the measurement is achieved. The CP gain is relatively stable across the 3 dB AR band, and its value ranges from 4.0 dBic to 4.2 dBic. The 3 dB AR bandwidth is 10 MHz. The designed antenna has the peak gain at the frequency where the AR value is the lowest. The deteriorative antenna circular polarization performance will worsen the antenna gain. Although the measurement in general agrees well with the simulation as

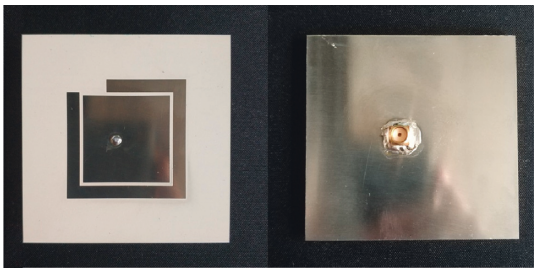

Figure 12: The fabricated CP microstrip antenna with the C-shaped parasitic strip.

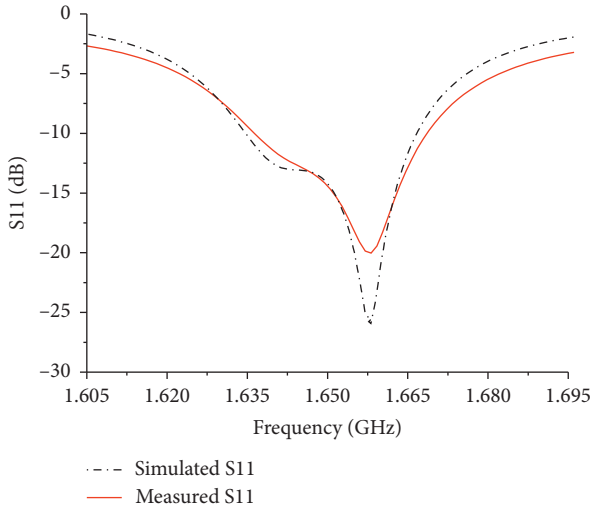

Figure 13: The simulated and measured S11 of the proposed CP microstrip antenna.

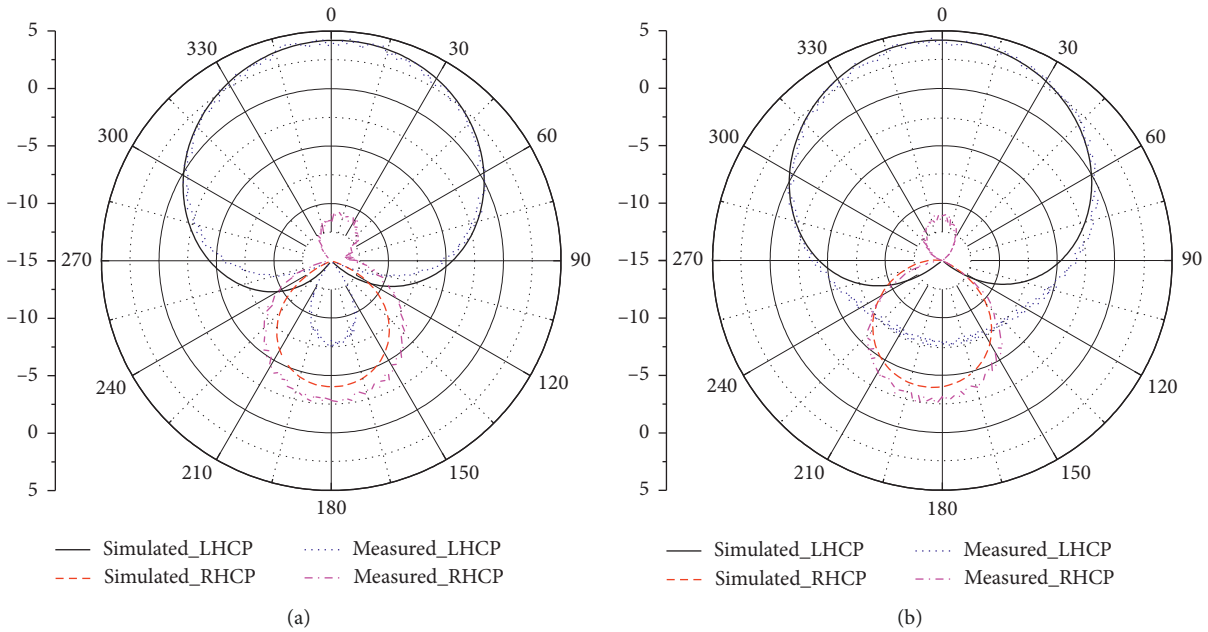

Figure 14: Measured and simulated antenna radiation patterns in the (a) phi = 0 deg and (b) phi = 90 deg planes.

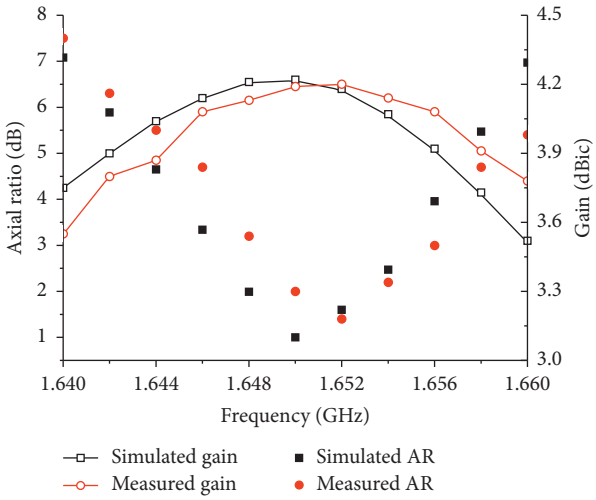

FIGURE 15: The ARs and CP gains versus frequency at the boresight direction.

observed in the figure, their differences may be due to the machine error and measurement error of the fabricated CP antenna.

6. Conclusions

A new single-feed CP microstrip antenna achieved by the C-shaped parasitic strip is proposed in this paper. The antenna CP characteristic is realized by adjusting the parasitic strip dimension. The microstrip antenna is fabricated based on the optimized parameter values. Bandwidth of the proposed CP antenna is approximately 30 MHz (1.8% with center frequency 1.65 GHz). The proposed CP microstrip antenna has approximately 4.2 dBic peak gain, 90deg 3 dB beamwidth, and 78% antenna efficiency. Moreover, the CP gain is relatively stable across the 3 dB AR band, and its value ranges from 4.0 dBic to 4.2 dBic. The main advantage and novelty of the designed CP antenna is that those two resonant modes for achieving the CP operation are independent from each other, which is convenient for the CP antenna design and debug.

Data Availability

The data used to support the findings of this study are currently under embargo while the research findings are commercialized. Requests for data, 12 months after publication of this article, will be considered by the corresponding author.

Conflicts of Interest

The authors declare that they have no conflicts of interest.

Acknowledgments

This work was supported in part by the National Natural Science Foundation of China (nos. 61771404 and 61601372). This work was also supported by the China Postdoctoral Science Foundation (no. 2018M631258) and the Postdoctoral Innovative Talent Support Program (no. BX20180003).

References

[1] K. Wei and B.-C. Zhu, "The novel W parasitic strip for the circularly polarized microstrip antennas design and the mutual coupling reduction between them," *IEEE Transactions on Antennas and Propagation*, vol. 67, no. 2, pp. 804–813, 2019.

[2] W.-J. Chen, H.-H. Chen, C.-H. Lee, and C.-I. G. Hsu, "Differentially fed wideband circularly polarized slot antenna," *IEEE Transactions on Antennas and Propagation*, vol. 67, no. 3, pp. 1941–1945, 2019.

[3] K. A. Yinusa, "A dual-band conformal antenna for GNSS applications in small cylindrical structures," *IEEE Antennas and Wireless Propagation Letters*, vol. 17, no. 6, pp. 1056–1059, 2018.

[4] Z.-X. Liang, D.-C. Yang, X.-C. Wei, and E.-P. Li, "Dual-band dual circularly polarized microstrip antenna with two eccentric rings and an arc-shaped conducting strip," *IEEE Antennas and Wireless Propagation Letters*, vol. 15, pp. 834–837, 2016.

[5] V. V. Reddy and N. V. S. N. Sarma, "Compact circularly polarized asymmetrical fractal boundary microstrip antenna for wireless applications," *IEEE Antennas and Wireless Propagation Letters*, vol. 13, pp. 118–121, 2014.

[6] V. V. Reddy and N. V. S. N. Sarma, "Triband circularly polarized koch fractal boundary microstrip antenna," *IEEE Antennas and Wireless Propagation Letters*, vol. 13, pp. 1057–1060, 2014.

[7] X. Zhang and L. Zhu, "High-gain circularly polarized microstrip patch antenna with loading of shorting pins," *IEEE Transactions on Antennas and Propagation*, vol. 64, no. 6, pp. 2172–2178, 2016.

[8] Nasimuddin, N. C. Zhi, and Q. Xianming, "Asymmetric-circular shaped slotted microstrip antennas for circular polarization and RFID applications," *IEEE Trans. Antennas Propag*, vol. 58, no. 12, pp. 3821–3828, 2010.

[9] H. Yang, Y. Fan, and X. Liu, "A compact dual-band stacked patch antenna with dual circular polarizations for BeiDou navigation satellite systems," *IEEE Antennas and Wireless Propagation Letters*, vol. 18, no. 7, pp. 1472–1476, 2019.

[10] Y. Shi and J. Liu, "A circularly polarized octagon-star-shaped microstrip patch antenna with conical radiation pattern," *IEEE Transactions on Antennas and Propagation*, vol. 66, no. 4, pp. 2073–2078, 2018.

[11] K. M. Mak, H. W. Lai, K. M. Luk, and K. L. Ho, "Polarization reconfigurable circular patch antenna with a C-shaped," *IEEE Transactions on Antennas and Propagation*, vol. 65, no. 3, pp. 1388–1392, 2017.

[12] C. Sun, Z. Wu, and B. Bai, "A novel compact wideband patch antenna for GNSS application," *IEEE Transactions on Antennas and Propagation*, vol. 65, no. 12, pp. 7334–7339, 2017.

[13] K.-K. Zheng and Q.-X. Chu, "A novel annular slotted center-fed BeiDou antenna with a stable phase center," *IEEE Antennas and Wireless Propagation Letters*, vol. 17, no. 3, pp. 364–367, 2018.

[14] K. Ding, C. Gao, D. Qu, and Q. Yin, "Compact broadband circularly polarized antenna with parasitic patches," *IEEE Transactions on Antennas and Propagation*, vol. 65, no. 9, pp. 4854–4857, 2017.

[15] Y.-Q. Zhang, X. Li, L. Yang, and S.-X. Gong, "Dual-band circularly polarized annular-ring microstrip antenna for

GNSS applications," *IEEE Antennas and Wireless Propagation Letters*, vol. 12, pp. 615–618, 2013.

[16] A. K. Gautam, A. Kunwar, and B. K. Kanaujia, "Circularly polarized arrowhead-shape slotted microstrip antenna," *IEEE Antennas and Wireless Propagation Letters*, vol. 13, pp. 471–474, 2014.

[17] X. Bai, X. Liang, M. Li, B. Zhou, J. Geng, and R. Jin, "Dual-circularly polarized conical-beam microstrip antenna," *IEEE Antennas and Wireless Propagation Letters*, vol. 14, pp. 482–485, 2015.

[18] K. Wei, J. Y. Li, L. Wang, R. Xu, and Z. J. Xing, "A new technique to design circularly polarized microstrip antenna by fractal defected ground structure," *IEEE Transactions on Antennas and Propagation*, vol. 65, no. 7, pp. 3721–3725, 2017.

[19] H.-D. Chen, S.-H. Kuo, C.-Y.-D. Sim, and C.-H. Tsai, "Coupling-feed circularly polarized RFID tag antenna mountable on metallic surface," *IEEE Transactions on Antennas and Propagation*, vol. 60, no. 5, pp. 2166–2174, 2012.

[20] G. Byun and H. Choo, "Antenna polarisation adjustment for microstrip patch antennas using parasitic elements," *Electronics Letters*, vol. 51, no. 14, pp. 1046–1048, 2015.